

---

# SYSTEMATIC ANALYSIS REVEALS KEY MICRORNAs AS DIAGNOSTIC AND PROGNOSTIC FACTORS IN PROGRESSIVE STAGES OF LUNG CANCER

---

**Dietrich Kong** <sup>†</sup>

Department of Computational Physics  
Institute of Modern Physics  
Chinese Academy of Sciences  
dietrichkong@gmail.com

**Ke Wang** <sup>†</sup>

Department of Computational Physics  
Institute of Modern Physics  
Chinese Academy of Sciences  
kvickywang@gmail.com

**Qiu-Ning Zhang**

Radiation medicine laboratory  
Institute of Modern Physics  
Chinese Academy of Sciences  
zhangqn@impcas.ac.cn

 **Zhi-Tong Bing** <sup>\*</sup>

Department of Computational Physics  
Institute of Modern Physics  
Chinese Academy of Sciences  
Advanced Energy Science and Technology  
Guangdong Laboratory  
bingzt@impcas.ac.cn

## ABSTRACT

MicroRNAs play an indispensable role in numerous biological processes ranging from organismic development to tumor progression. In oncology, these microRNAs constitute a fundamental regulation role in the pathology of cancer that provides the basis for probing into the influences on clinical features through transcriptome data. Previous work focused on machine learning (ML) for searching biomarkers in different cancer databases, but the functions of these biomarkers are fully not clear. Taking lung cancer as a prototype case of study. Through integrating clinical information into the transcripts expression data, we systematically analyzed the effect of microRNA on diagnostic and prognostic factors at deteriorative lung adenocarcinoma (LUAD). After dimension reduction, unsupervised hierarchical clustering was used to find the diagnostic factors which represent the unique expression patterns of microRNA at various patient's stages. In addition, we developed a classification framework, Light Gradient Boosting Machine (LightGBM) and SHAPley Additive explanation (SHAP) algorithm, to screen out the prognostic factors. Enrichment analyses show that the diagnostic and prognostic factors are not only enriched in cancer-related pathways, but also involved in many vital cellular signaling transduction and immune responses. These key microRNAs also impact the survival risk of LUAD patients at all (or a specific) stage(s) and some of them target some important Transcription Factors (TF). The key finding is that five microRNAs (hsa-mir-196b, hsa-mir-31, hsa-mir-891a, hsa-mir-34c, and hsa-mir-653) can then serve as not only potential diagnostic factors but also prognostic tools in the monitoring of lung cancer.

**Keywords** MicroRNA · Lung cancer · Machine learning · Clinical information

## 1 Introduction

Lung cancer is the leading cause of cancer-related human deaths worldwide [Sung et al., 2021]. Approximately 85% of the lung cancer cases can be classified as non small-cell lung cancer (NSCLC), among which lung adenocarcinoma (LUAD) is one of the most common subtypes [Segal et al., 2018]. The molecular mechanisms behind cancer evolution are

---

<sup>\*</sup>Corresponding Author. Email: bingzt@impcas.ac.cn

extremely complex, impeding accurate and reliable diagnosis and prognosis as well as effective treatment [Molina et al., 2008]. A milestone discovery the general developmental and disease contexts is the roles played by non-coding RNAs (ncRNAs) [Anastasiadou et al., 2018], especially microRNAs [Sayyed et al., 2021, Bartel, 2018, Gebert and MacRae, 2019, Chen et al., 2019]. In cancer research, at the RNA level, the microRNA has been found in key regulators of physiological functions and major cancer types [Aboutalebi et al., 2020, Wei et al., 2018, Luo et al., 2019, Hong et al., 2020, Zhang et al., 2021]. Particularly relevant to lung cancer, microRNA had been identified as the oncogenic drivers and tumor suppressors [Wu et al., 2019, Yan et al., 2018, Naeli et al., 2020, Pandey et al., 2021].

A standard existing approach to monitoring tumor progress and detecting/ascertaining the underlying mechanism is non-coding RNA transcriptomics, which has led to a large number of significant biomarkers and therapeutic targets [Seo et al., 2012, Network and Others, 2014, Epsi et al., 2019, Dama et al., 2021]. In previous studies of ncRNA, a commonly practiced methodology is to identify some Differentially Expressed (DE) RNAs based on absolute Fold Changes (FC) and values of the false positive ratio [Yu et al., 2019, Zhong et al., 2020, Yang et al., 2020]. Some recent works input ncRNAs expression data into machine learning (ML) algorithms [Lopez-Rincon et al., 2019, Farsi, 2021, Ma et al., 2020], such as LightGBM to seek markers. And others analyze how microRNA affects the prognosis of patients by combining clinical data [Asakura et al., 2020, Zhong et al., 2021, Xin et al., 2020].

These methods and analyses have inferred some microRNAs related to lung cancer and have been well verified, but there has been little systematic discussion of the relationship between diagnostic factors and prognostic factors. Nonetheless, it is unlikely that the intrinsic molecular remain static during cancer development, the dynamical interplay among various prognosis and diagnosis functions of RNAs was completely ignored. To better understand cancer and to identify more effective factors, the dynamical aspects of the ncRNA in LUAD must be taken into account. To remedy this deficiency had motivated our work. With the presently available gene expression and clinical information, we were able to incorporate investigation of diagnosis and prognosis of lung cancer. In particular, we focused on the three stages of LUAD progression based on both transcriptome and corresponding clinical data of LUAD from The Cancer Genome Atlas<sup>2</sup>.

Through selecting the unique pattern from hierarchical clustering of microRNA expression in each given stage of LUAD, we found that some microRNAs were potentially served as diagnostic factors with cancer stages. And proved that the expression pattern of these diagnostic factors does not directly correspond to the molecular characteristics, such as gene expression, FC value, and even survival risk variables. In addition, we classified the LUAD samples of each stage into two categories based on survival differences and employed an efficient and stable LightGBM algorithm to train the microRNA expression data with binary labels in the three stages of LUAD respectively. Then a SHAP algorithm was applied to explain the mechanism of the ML classifiers and verify key prognostic factors.

Performing the Kyoto Encyclopedia of Genes and Genomes (KEGG) pathway enrichment analyses of those diagnosis or prognosis factors, we found that these factors are involved in a wide range of cancer-related pathways and related to important signaling translation pathways and immune processes. Finally, we carried out K-M survival curve analysis and constructed the regulation network of factors and their targeted Transcription Factors (TF). Our work established a more comprehensive diagnosis-prognosis framework than previous ones, not only providing tools to probe more deeply into the mechanisms of cancer evolution than previously possible but also having the potential to lead to more effective drug targets for LUAD as well as other types of cancer.

## 2 Results

### 2.1 Differential Expression (DE) Analysis and Confirmation of Biological Function

#### 2.1.1 DE microRNAs

As described in **Materials and Methods**, to explore there lationship between diagnosis and prognosis in evolutionary carcinoma, we first obtained the DE RNAs by comparing the microRNAs expression values in the LUAD samples with those from the normal samples. The amounts of samples and DE microRNAs in each stage were shown in Supplementary Table 1.

In the volcano map, Figure 1A, some of the microRNAs with significant FC and P-value ( $-\log_{10}(P) > 20$ ,  $\log_2|FC| > 2$ ) have been widely reported, such as microRNAs hsa-mir-21, hsa-mir-9, etc. [Liu et al., 2010, Guinde et al., 2018]. However, DE analysis cannot select those molecules with smaller FC values, but they may play a vital role. We hoped to understand the molecular mechanism of evolutionary cancer not only from statistical indicators (FC value) of transcripts expression but also from other dimensions through systematical analysis. Therefore, a loose threshold was chosen in the process of DE analysis ( $P - value < 0.05$ ,  $\log_2|FC| \geq 1$ ) so as to avoid significant molecules being abandoned,

<sup>2</sup><https://portal.gdc.cancer.gov/>

and finally 127, 130, and 131 microRNAs were selected in the early, middle, and later stages correspondingly, as shown in Figure 1B.

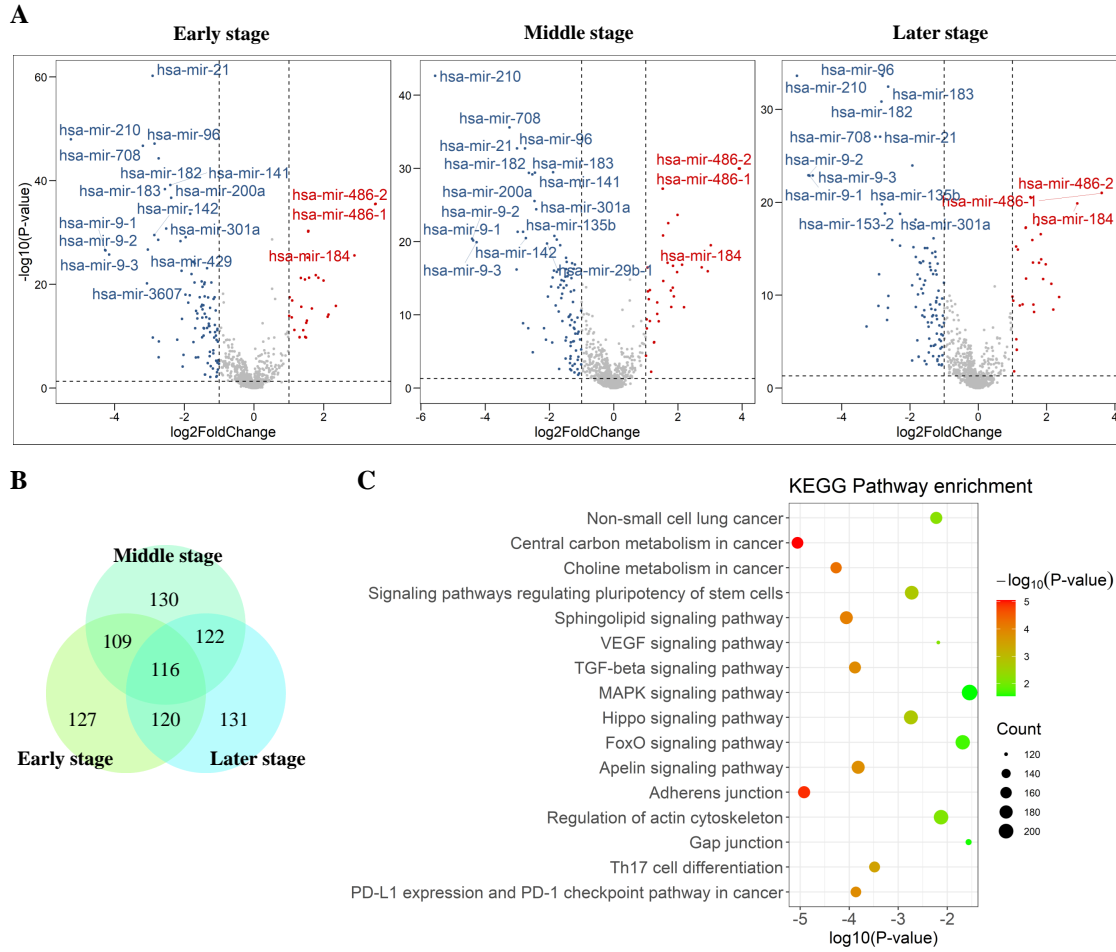


**Figure 1: Differentially expressed microRNAs and their functions in LUAD.** A. Volcano maps of the microRNA expression in early, middle, and later stages of LUAD samples. The  $x$ -axis is  $\log_2$  FC (FC value), and the  $y$ -axis is the  $-\log_{10} P$  from the DE analysis. We selected the threshold  $P < 0.05$  and  $\log_2$  FC  $> 1$ , especially, these microRNAs which meet the threshold  $-\log_{10} P > 20$  and  $\log_2$  FC  $> 2$  were labeled by names. B. The Venn diagram illustrates the number of DE microRNAs in different stages of LUAD, reflecting molecules in the dynamical LUAD have a very high level of overlap. C. The KEGG pathway enrichment analysis was performed on DE microRNAs. It revealed that these microRNAs are closely related to the biological functions of the cancer pathway, signal Translational, and immune pathway.

### 2.1.2 Confirmation of Biological Function

The current understanding of the biological functions of microRNAs is far less than coding protein messenger RNA, and little is known about the precursor microRNA. Considering that the content of precursor microRNA in organisms can be reflected in the amount of mature microRNAs in cells or tissues to a certain extent [Liu et al., 2016]. So the biological pathway enrichment analysis of mature microRNAs was used to confirm the potential biological function of their precursor.

According to the results of KEGG enrichment analysis in Figure 1C, the DE precursor microRNAs are not only enriched in cancer-related pathways, such as “MicroRNAs in cancer”, “Non-small cell lung cancer” and “Transcriptional misregulation in cancer”. It also involves many biological signaling pathways, such as Proteoglycans, Central carbon metabolism, Choline metabolism in cancer and the TGF- $\beta$ /MAPK pathways. In addition, it plays a role in immune-related and other biological processes such as Th17 cell differentiation, cell adhesion, and motor protein. In addition,

the microRNA enrichment pathways in different the various LUAD stages were also analyzed (shown in Supplementary Figure 1).

## 2.2 Diagnostic Factors in Different LUAD Stages

### 2.2.1 The expression information being stored in the eigenvector

In order to explore which of the DE microRNAs are suitable as diagnostic factors of the dynamical LUAD stages based on TNM classification (see **Materials and Methods** for the meaning of TNM). We first reduced the dimensionality of the microRNA expression data to eliminate possible gene expression noise in the transcriptome data. The size of sample-microRNA expression matrices in the three stages of LUAD are (273, 127), (120, 130), and (103, 131), respectively. For these three matrices, we first decentralized it and calculated the covariance matrix, and then performed eigenvalue decomposition (**Materials and Methods** for more details). The 90% information of microRNA expression data was retained, and finally, 30, 26, and 25 eigenvalues were selected in the early, middle, and later stages of LUAD patients.

### 2.2.2 Eigenvector independent with expression and clinical characteristics

The Pearson correlation coefficients between eigenvector weight and RNA expression or FC value are within plus or minus 0.3, as shown in Supplementary Figure 2. Therefore, the numerical value of the eigenvector does not depend on the statistical indicators related to gene expression. This analysis may ensure that the subsequent process to identify the clinical function of microRNAs is all to a great extent independent of microRNA expression.

In addition, considering that the eigenvectors may be related to survival, rather than specific diagnostic factors of each stage, we employed the Cox proportional hazard regression model (in Supplementary Note 2) to calculate the Hazard Risk of eigenvectors and compare the two typical clinical characteristics, age and gender separately (in Supplementary Table 3). It's not the top eigenvectors that have the greatest impact on survival ( $p < 0.05$  and  $|HR - 1| > 0.1$ ), indicating that the data reduction process for finding diagnostic factors does not depend on patient survival information (in Supplementary Table 3). And thus the expression of DE microRNAs and survival data are statistically independent.

### 2.2.3 Unique expression patterns of microRNA

Molecules served as a kind of diagnostic factors possess unique gene expression characteristics in each the gene expression of microRNAs should be potentially stages of LUAD, so the microRNAs with the distinguished pattern of the gene expression should be potentially considered as the stage-based diagnostic factors. What's more, clustering by the value of the microRNA expression corresponding to the eigenvector load is beneficial for finding molecules with abnormal expression patterns in the data structure itself, rather than just directly looking for the gene expression characteristics.

### 2.2.4 Hierarchical clustering of microRNAs expression

Figure 2 depicts the results of unsupervised hierarchical clustering of microRNAs expression eigenvectors with three LUAD stages. Each molecule was classified into a group according to its Euclidean distance, and this process was repeated until all molecules are gathered into the same super-category. The molecular expression patterns within clusters are similar, while the differences between various clusters are large. The greater the distance from left to right in the clustering diagram Figure 2, the more different the expression patterns of the sub-categories. The left sub-categories (colored) have a larger difference compared with the overall categories on the right (gray). Therefore, the gray part on the right side of the figure is a group of microRNAs with very similar expression patterns, while the left side is a number of molecules with relatively more varied expression patterns and thus those molecule(s) can be seen as a single category.

In the meantime, we calculated clustering height which is a measure of discrimination for microRNA expression patterns, illustrated in the top-right line graphs (Figure 2). In particular, we ranked the spatial Euclidean distances between a cluster of microRNA(s) and other all clusters, and the largest difference of it was marked by the red dotted line which was used as the threshold. Finally, the top 9, 13, and 12 clusters were screened out in the early, middle, and later LUAD stages. Therefore, we extracted those microRNA with unique expression patterns in each LUAD stage separately (Figure 2).

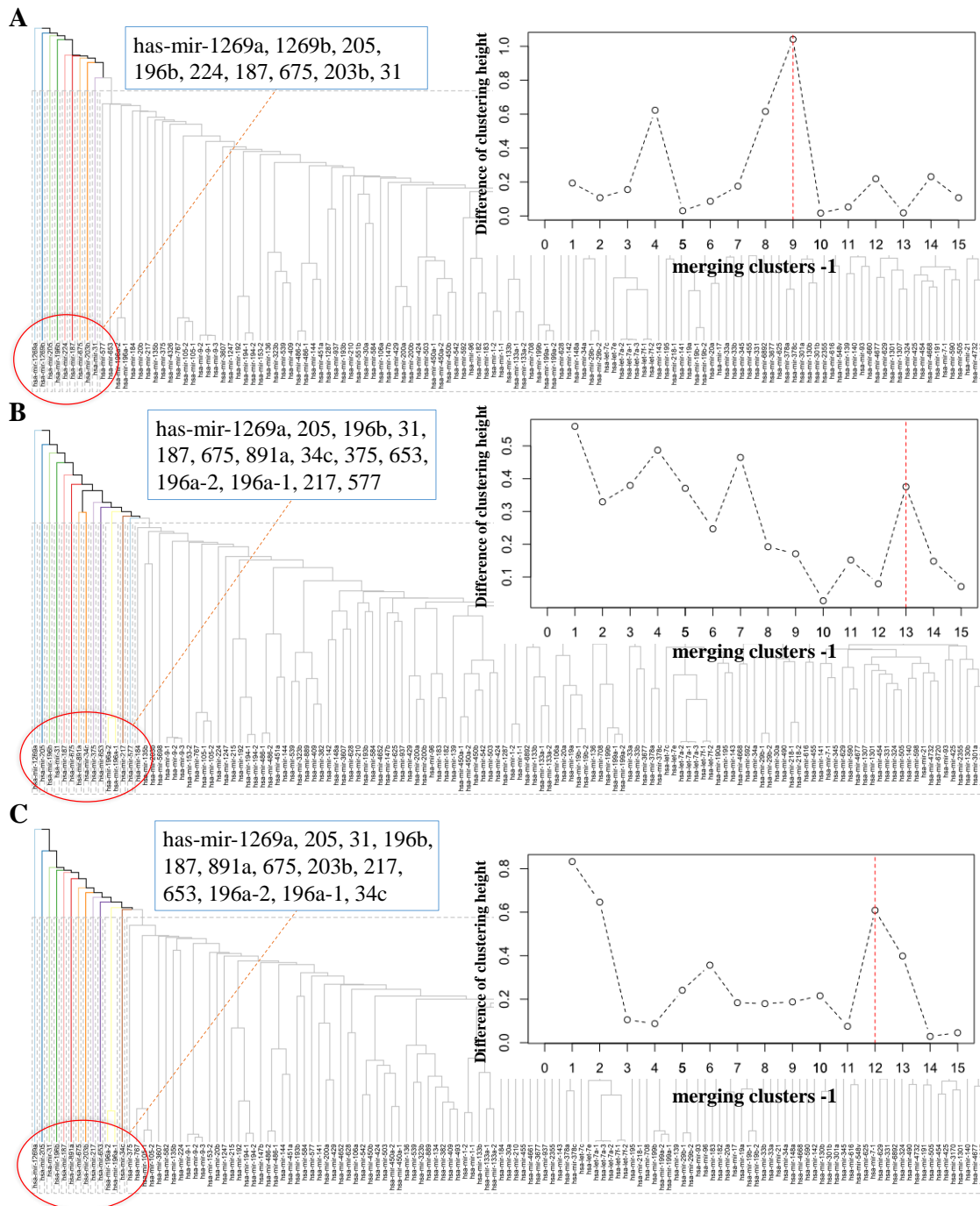


Figure 2: **Clustering analysis for diagnostic factors of three LUAD stages.** The unsupervised hierarchical clustering of microRNA expression eigenvectors was shown in A. early, B. middle, and C. later LUAD stages. Compared with the right part (gray) which is a group of microRNAs with a very similar expression, the color part on the left has a relatively more varied expression pattern, so these molecules have a greater degree of changes of expression with each other. The greater the distance from left to right in the clustering graph, the more different the expression patterns of “sub-categories”. The line graph at the top-right depicted clustering height (spatial Euclidean distance) between each different microRNA cluster in a given stage of LUAD. The red dotted lines indicate that 9, 13, and 12 are suitable criteria for the top 15 clusters. The total number of microRNAs are 127, 130, and 134 in three stages respectively.

### 2.2.5 Diagnostic factors with independent characteristics

Finally, We screened out 9, 14, and 13 microRNAs (More details in The blue rectangular box in Figure 2) respectively that could be considered as diagnostic factors in early, middle, and later LUAD stages. It is worth mentioning that these microRNAs are totally not similar with significant microRNA ( $-\log_{10}(P - value) > 20$ ,  $\log_2|FC| > 2$ ) from DE analysis at each LUAD stage. For example, the gene expression pattern of has-mir-1269a is distinctive from other molecules, but its expression and FC value (Figure 1A) are not significant.

In short, by the dimensionality reduction and unsupervised hierarchical clustering, the microRNAs that we obtained with specific unique expression patterns in each stage, therefore, can be reasonably regarded as diagnostic factors which are independent from gene expression, FC Value, and survival risk in the evolution of LUAD.

## 2.3 Prognostic Factors in Progressive Stages of LUAD

### 2.3.1 Data preprocessing and feature dimensionality reduction

Samples from each stage were classified to identify patient groups with differences in survival, but a significant portion of the follow-up data from clinical survival data was lost and there was no final patient survival time. To facilitate accurate identification of prognostic molecules of cancer without being disturbed by the missing clinical sample information, we only selected patient data with complete survival information for prognostic factors analysis (see Supplementary Table 2 for details). Considering that this kind of high-dimensional data still has many molecular characteristics even after DE analysis, those samples for commonly used ML classification algorithms are extremely insufficient. Therefore, for the purpose of finding prognostic factors, we used mutual information [Kraskov et al., 2004, Ross, 2014, Kozachenko and Leonenko, 1987] to screen out the features unrelated to the survival of patients. In the three LUAD stages of microRNA expression data, 57, 66, and 51 molecules were screened to determine the survival probability of the patient.

### 2.3.2 LightGBM models and SHAP algorithm

Prognostic factors are closely related to the survival time of patients. For the purpose of exploring which biomolecules can affect the prognosis with lung cancer, a ML algorithm LightGBM [Ke et al., 2017, Quinto, 2020, Ahn et al., 2021, Dong et al., 2020] was applied to predict the survival time of patients. Based on the gene expression data of microRNA, we constructed binary classifiers of the survival time in the early, middle, and later stages of LUAD. To characterize the importance of various molecules in a specific classifier, the SHAP value [Lundberg et al., 2018, 2020] was measured. At the same time, to better estimate the performance of the model, we used the 10-fold cross-validation training method. In this research, ACC and AUC are both the average results of the test sets in 10-fold cross-validation, as shown in Figure 3.

Specifically, we first trained the binary LightGBM prediction models based on microRNA expression data, with AUC values of 0.62, 0.68, and 0.68 in three stages of LUAD, as shown in Table 1.

Table 1: The performance of 10-fold cross-validation of LightGBM classifier in LUAD three stges.

	Round	Num. of factors	ACC	AUC
Early stage	1	57	0.70	0.62
	2	12	0.83	0.77
	3	8	0.86	0.81
Middle stage	1	66	0.71	0.68
	2	22	0.89	0.87
	3	12	0.88	0.88
Later stage	1	51	0.67	0.68
	2	8	0.82	0.83
	3	7	0.85	0.87

In order to further optimize the model and improve its performance, we calculated the contribution of each molecule to the model accuracy by SHAP algorithm and selected the top k microRNAs for a new round of classifiers training. Then, by comparing the performance of different classifiers, we acquired 12, 22, and 8 molecules (AUC: 0.77, 0.87, and 0.83) in the sequential three stages of LUAD, which were significantly higher than the performance of the previous model. In this round, the new classification models were evaluated, and the top 8, 12, and 7 molecules were again filtered out according to the SHAP value. Finally, the AUC of the classification models reached 0.81, 0.88, and 0.87 respectively.

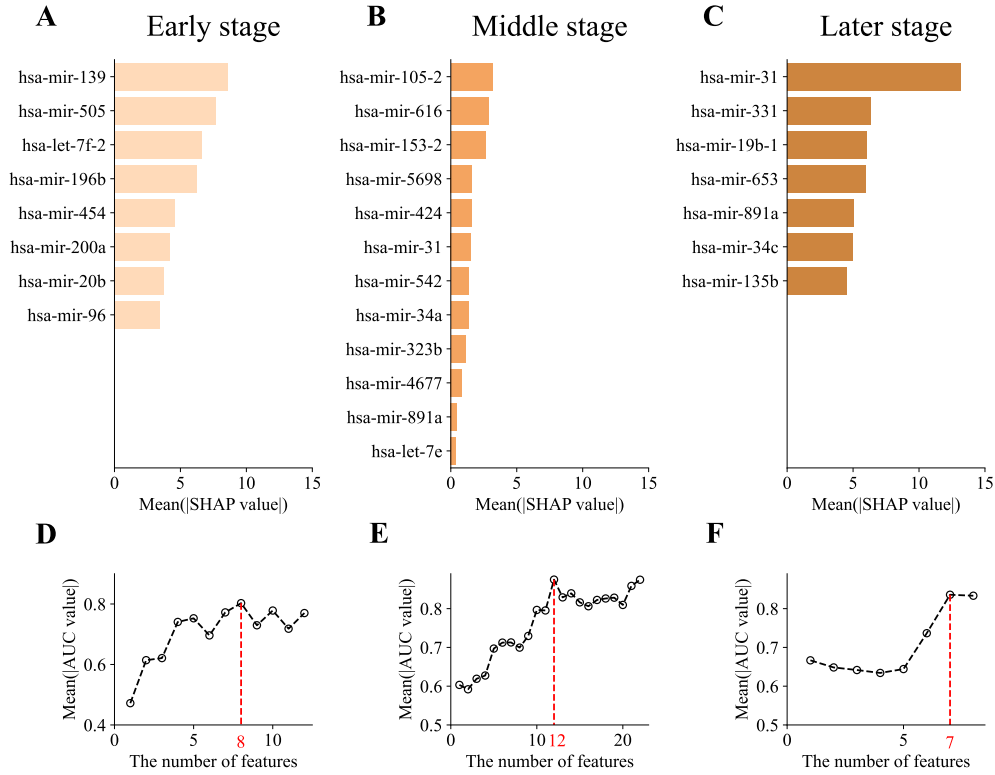


Figure 3: **SHAP values of prognostic factors in three stages of LUAD.** The prognostic factors obtained after 3 rounds of classifier training and their corresponding contributions (SHAP value) to the model were displayed from high to low in the A. Early, B. Middle, and C. Later stages of LUAD. The following line charts (D. Early, E. Middle, and F. Later.) described the average AUC value of the classifier in the 10-fold cross-validation when the top k features were selected in the round 2 model. The red dotted line indicates that the model performs best when k is 8, 12, and 7 respectively.

And when continuing to optimize the model with the interpretable methods, we found the classifier performance couldn't be improved by further reducing the number of microRNAs. So, we obtained three binary classifiers and got the microRNA molecules which are the key factors affecting the survival time of patients and potentially used to measure the prognosis according to the microRNA expression data with early, middle and later LUAD.

### 2.3.3 Relationship between algorithm indexes and characteristics of gene expression

It is worth mentioning that in the second round of classifier models, we carefully analyzed the gene expression characteristics of those molecules, and explored the bioinformatics significance of this ML method. These LUAD-related top prognostic factors obtained from the binary classification model are independent variables from their expression characteristics, such as microRNA expression level or FC value Supplementary Figure 3.

## 2.4 Key Diagnostic and Prognostic Factors

### 2.4.1 The dynamical interaction of diagnosis and prognosis factors in evolutionary LUAD

We have developed two methods to find potential microRNAs which can be served as diagnostic and prognostic factors in the evolution of LUAD. Because there is no mechanism introduced in our methods process to exclude the distribution of biomarkers in various stages of cancer, usually there are some overlap biomarkers in different stages. In Figure 4 A and B, the six microRNAs hsa-mir-1269a, hsa-mir-205, hsa-mir-196b, hsa-mir-187, hsa-mir-675, and hsa-mir-31 are used as diagnostic factors shared with the three stages of LUAD. However, there is no overlap of the prognostic factors in all LUAD stages.



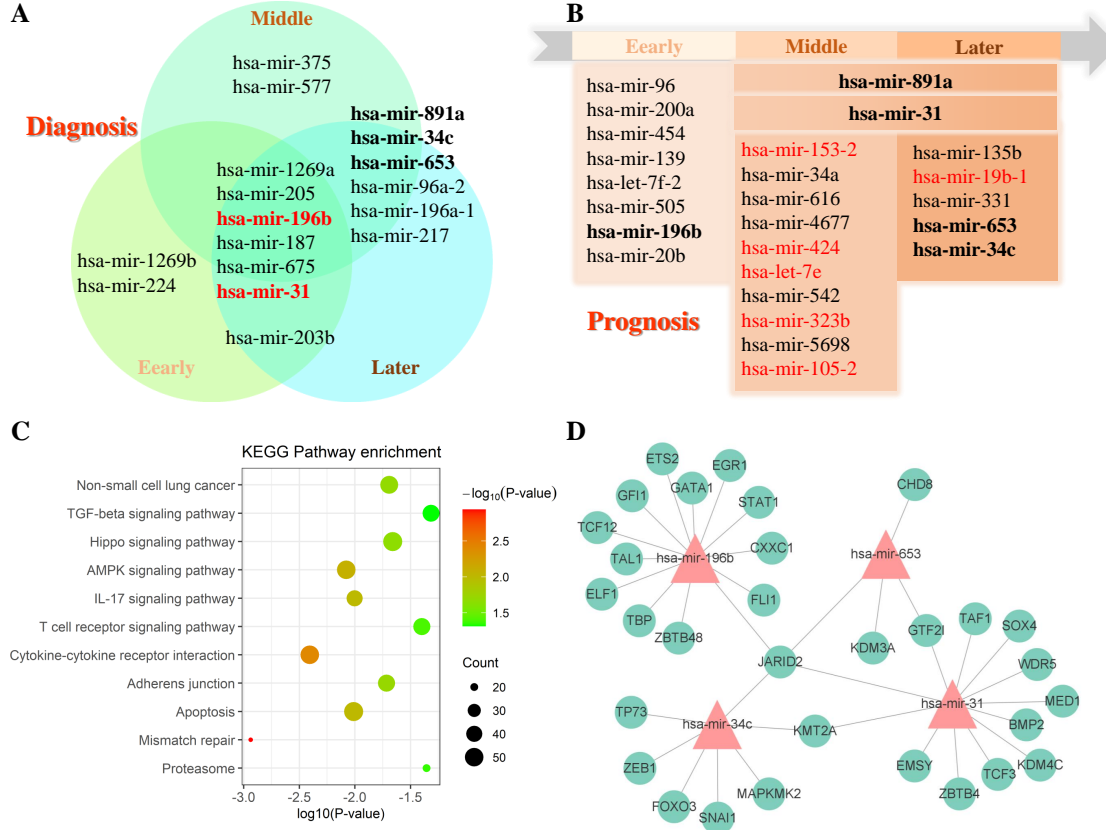


Figure 4: **The key diagnostic and prognostic factors with the evolutionary LUAD.** A. The diagnostic factors for LUAD stages were shown in a Venn diagram. B. An overall diagram of key prognostic factors in three stages of LUAD. The molecules in bold are both shared in diagnostic and prognostic factors, and those in red have an effect on patient survival. The diagnostic factors in the dynamical LUAD have a very high-level overlap in various stages. C. Those final microRNAs served as diagnostic factors in different LAUD stages were significantly enriched in some pivotal cancer-related KEGG pathways. D. The microRNA-TF interaction network, where the microRNAs belong to both diagnostic and prognostic factors in our analyses.

In addition, the prognostic and diagnostic factors relatively overlap in the middle and later stages in the evolution of the classification of LUAD samples. However, the early stage of TNM staging (Stage I) is indeed different from the later stage (stage III and IV). To be specific, in the prognostic factors, hsa-mir-891a and hsa-mir-31 exist in both middle- and later-stage, while no molecule is the same in the early stage as that in the remaining two stages. For the biomarkers of different stages, between the middle- and later-stage, it contains many common biomarkers, such as hsa-mir-891a, hsa-mir-34c, hsa-mir-653, hsa-mir-196a-2, hsa-mir-196a-1, hsa-mir-217. In contrast, there is only the intersection of hsa-mir-203b in the early- and the later-stage, and even no common molecule with middle stage.

It's worth noting that the five microRNAs of hsa-mir-196b, hsa-mir-31, hsa-mir-891a, hsa-mir-34c, and hsa-mir-653 in the three stages of LUAD evolution are not only used as diagnostic factors but also as prognostic factors. Among them, hsa-mir-31 and hsa-mir-196b as diagnosis of all stages of LUAD can influence the survival of patients in the early- and later-stage Figure 5E and F.

#### 2.4.2 Molecular heterogeneity of Stage II

Generally, since changes of TNM pathological characteristics are continuous during deteriorative cancer, it cannot well distinguish the biomarkers in different stages of LUAD by the analysis of the gene expression data of microRNA transcripts. This is consistent with the conclusion of the difference between the clinical classification and biomolecular characteristics of the cancer stage. In the meantime, we also found that the heterogeneity of the second stage may be relatively high, this phenomenon is also consistent with the previous study [Wu et al., 2019, Rudin et al., 2021]. Detailed, in our research, the number of prognostic microRNAs in stage II is larger and their SHAP value are relatively



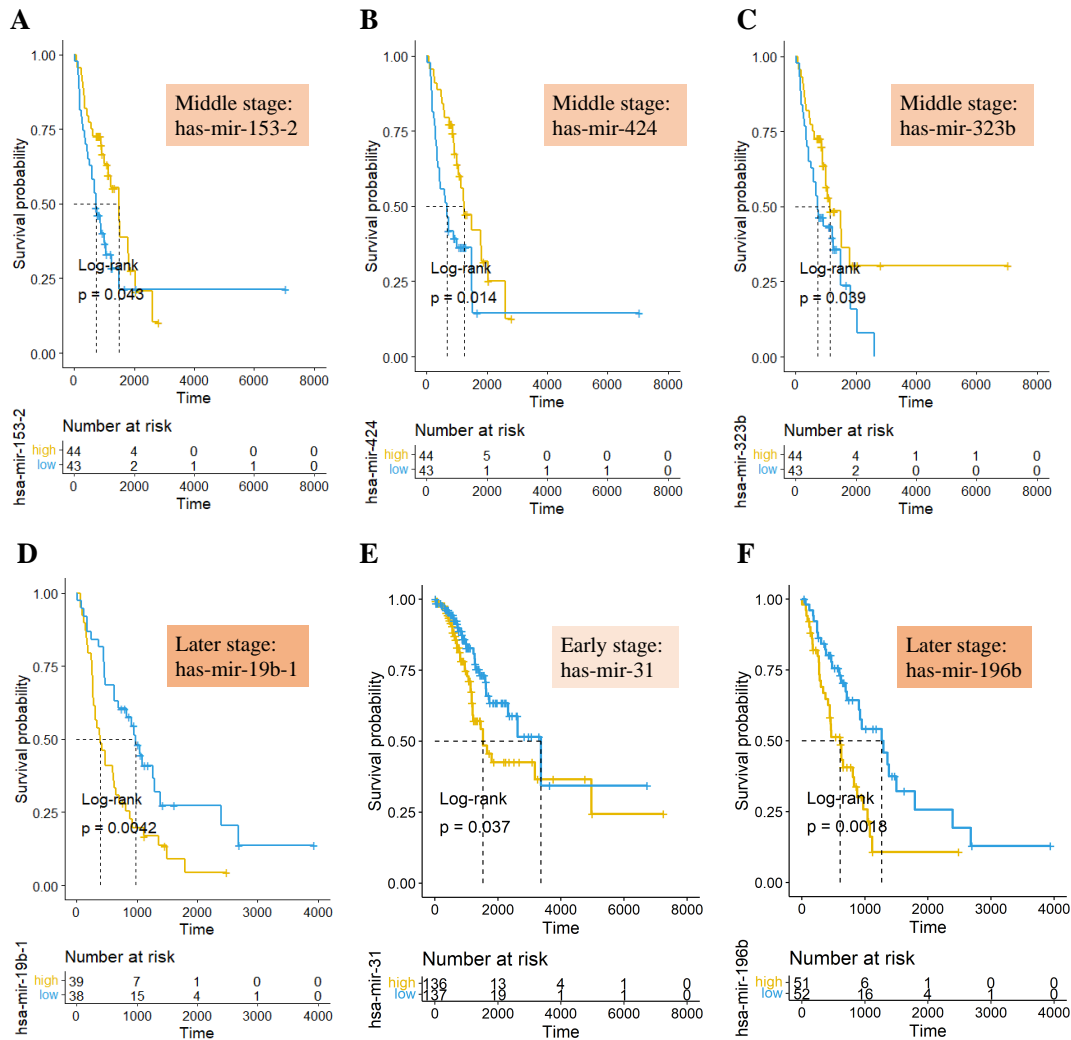


**Figure 5: MicroRNAs that affect patient survival.** The Kaplan-Meier analysis showed that the key microRNAs (four of prognostic factors and two of diagnostic factors) have a significant influence on patient survival in a specific LUAD stage. Log-rank tests were used to analyze the Kaplan-Meier survival curve.

smaller compared with other stages. Besides, the variance of eigenvector clustering height in the middle stage of LUAD (see Figure 2B) is larger which indicates a high degree of similarity within the clustering groups.

### 2.4.3 Functional validation of precursor microRNAs

What is the function of those stem-loop microRNAs mined from lung cancer? To address this question, we performed KEGG pathway enrichment analysis of mature microRNA corresponding to the precursor microRNA in our LUAD data. (Supplementary File 1 presents more details of the enrichment analysis of those precursor microRNAs.) The result displays that the biomarkers of microRNAs are strongly correlated with cancer-related pathways, such as Non-small cell lung cancer ( $-\log_{10} P > 20$ ). Besides, it is also mainly related to signal transduction and cellular immune functions, such as hsa-mir-196b, hsa-mir-31, hsa-mir-34c, hsa-mir-891a, etc. being involved in “Non-small cell lung cancer,” “TGF-beta signaling pathway,” “Hippo signaling pathway,” and “AMPK signaling pathway”. In addition, these microRNAs also work with “IL-17 signaling pathway,” “T cell receptor signaling pathway,” “Cytokine-cytokine receptor interaction,” and other immune pathways are related, and may also be related to “Apoptosis,” “Adherens junction,” “Mismatch repair,” and “Proteasome biological process”.

Taken together, the enrichment analysis of microRNAs reveals that our reconstructed diagnosis and prognosis factors exhibit a close correspondence to the development of LUAD and deterioration of physiological indicators from early- to later-stage, validating our systematic analysis method.

#### 2.4.4 MicroRNA targeted TF network

A very important part of the regulatory mechanism of microRNA is to regulate the transcription process by forming a complex with the protein-encoding mRNA or protein that participates in the DNA trans regulation [Wu et al., 2019]. Therefore, we had also investigated the interaction between microRNAs and transcription factors (TF) and found that some molecules are closely related to cancer, which shed light on the regulatory mechanism of a microRNA to control cancer progression, as shown in Figure 4D.

JARID2 encodes a Jumonji- and AT-rich interaction domain (ARID)-domain-containing protein. The encoded protein is a DNA-binding protein that functions as a transcriptional repressor. It regulates gene expression, but the precursor RNA mainly accumulates in the nucleus, which can also be combined with transcription factors to regulate the process of gene expression. This gene functions as a node gene for hsa-mir-196b, hsa-mir-31, hsa-mir-34c, and hsa-mir-653. We noticed that hsa-mir-196b interacts with EGR1, which is closely related to cancer [Li et al., 2018, Huang et al., 2020b, Liang et al., 2020], and hsa-mir-31 is involved in the key gene SOX4 which may function in the apoptosis pathway leading to cell death as well as to tumorigenesis [Hanieh et al., 2020, Hou et al., 2016, Edmonds et al., 2016].

And hsa-mir-34c is related to the FOXO3 gene, which belongs to the forkhead family of TFs and likely functions as a trigger for apoptosis through the expression of genes necessary for cell death [Huang et al., 2020a, Li et al., 2014]. Both hsa-mir-31 and hsa-mir-34c can target KMT2A protein. This gene encodes a transcriptional coactivator that plays an essential role in regulating gene expression during early development and hematopoiesis [Safran et al., 2010]. The encoded protein contains conserved functional domains SET which is responsible for its histone H3 lysine 4 (H3K4) methyltransferase activity which mediates chromatin modifications associated with epigenetic transcriptional activation [Safran et al., 2010]. The Gene Ontology (GO) annotations related to GTF2I (General Transcription Factor Ii) include DNA-binding transcription factor activity and mitogen-activated protein kinase binding. Among its related pathways are Assembly of RNA Polymerase-II Initiation Complex and Akt Signaling. Nevertheless, co-targeting of GTF2I from the precursor microRNA hsa-mir-31 and hsa-mir-653 may be connected with cancer in our network. Supplementary File 2 and 3 present more details of the possible pathological associations of these key microRNAs as diagnostic and prognostic factors dated from the knowledge database [Xie et al., 2013, Huang et al., 2019].

#### 2.4.5 MicroRNAs with a significant influence on patient survival

Combining the microRNA gene expression data and the survival data of the samples during the evolution of lung cancer, we performed the K-M survival analysis [Kaplan and Meier, 1958, Kaplan, 1983] to study the relationship between these molecules and patient survival. The results showed that hsa-mir-153-2 (P-value, 0.043), hsa-mir-424 (P-value, 0.014), hsa-mir-323b (P-value, 0.039) significantly affects the survival of the middle stage samples Figure 5, while hsa-mir-19b-1 (P-value, 0.0042) has a significant effect on survival of later samples. Figure 5 A-C. hsa-mir-31 (P-value, 0.0037) and hsa-mir-196b (P-value, 0.0018), as all-stage diagnostic factors, can affect the survival rate of patients in the early- and later-stage respectively Figure 5 E and F. In addition, several microRNAs affect the survival for all LUAD patients as shown in Supplementary Note 3 and Supplementary Figure 4.

### 3 Discussion

LUAD has more pronounced genomic variations [Vergoulis et al., 2011] than other lung cancer subtypes, which are rarely caused by a few genetic changes [Hsu et al., 2014], rendering necessary articulating alternative methodologies in order to obtain a reasonable understanding of the complicated mechanisms behind the evolution of cancer. In the past decades, it was widely believed that non-coding RNA had been involved in the regulation of gene expression and cancer occurrence and development. Analyses based on the transcriptome data of non-coding RNA provide a promising approach to understanding microRNA regulation at the post-transcriptional level [Xiao et al., 2008, Tay et al., 2014a, Adams et al., 2014]. Although some work studied how multiple types of molecular interactions affect cancer, such as CeRNA-related studies [Yu et al., 2019, Zhao et al., 2021] that match the relationship between endogenous competing RNAs to analyze biological functions and pathways closely related to lung cancer. Nevertheless, these studies ignore the tumor microenvironment and the accuracy of ceRNAs targeting genes.

Therefore, from a clinical pathology view, the effects of microRNA on the stage characteristics and prognosis of cancer patients were still not well understood. In order to simplify the problem without introducing certain biological hypotheses such as the CeRNA hypothesis [Ebert et al., 2007, Salmena et al., 2011, Tay et al., 2014b], but based on the

original transcriptome data. We hoped to comprehensively assess which molecules in the evolution of cancer are related to the patient's diagnosis and prognosis and how these key microRNAs evolve along with the lung cancer worsening. We systematically explored the relationship between the two functions of microRNA as the diagnostic and prognostic factors. Because of the limited sample cases and the high degree of molecular heterogeneity of cancer, it is infeasible to determine which methods are more suitable for finding biomarkers of LUAD in the process of microRNA transcriptional data. In our research, through a step-by-step method, combined with corresponding biological information and clinical data, we analyzed the microRNA expression data of LUAD patients in the early, middle, and later stages. Our analysis delineated the dynamical changes of these key microRNAs in the progression stages from early to later. Beyond that, high molecular heterogeneity was also observed in the middle stage.

By performing KEGG pathway enrichment analysis on mature microRNAs linked by precursor, we had identified those key underpinning RNA molecules that are not only directly involved in various cancer pathways but also signal transduction as well as immune-related pathway (Figure 4C). This is a strong indication that these microRNAs are involved in LUAD and its evolution. Especially, by targeting TF, we found that some specific oncogene in the microRNA and TF network (Figure 4D). Through the Kaplan-Meier survival analysis [Kaplan and Meier, 1958, Kaplan, 1983], we had also identified some key microRNAs that have a significant influence on the survival rate of LUAD patients (Figure 5). In a word, beyond the "static" information provided by the conventional gene ontology analysis of the four stages of LUAD, our framework of data process gives rise to a dynamic scenario for tumor progression as the TNM stage deteriorates.

In particular, five microRNAs markedly acted as the diagnostic factors of stage classification and prognostic factors of LUAD patients. The first is hsa-mir-196b reported in recent studies, which promotes lung cancer cell migration and invasion through the targeting of GATA6 [Li et al., 2018]. Another microRNA is hsa-mir-31, which is involved in the inhibition of specific tumor suppressants in human lung cancer [Kasinski and Slack, 2011], and some important signaling pathways about lung cancer [Edmonds et al., 2016, Hou et al., 2016]. The third one is hsa-mir-34c, which participates in promoting invasion and migration of non-small cell lung cancer (NSCLC) by upregulating integrin alpha 2 beta 1 [Huang et al., 2020a], and its homolog may be served as a therapeutic target in human cancer [Li et al., 2014]. Nevertheless, hsa-mir-891a and hsa-mir-653 have not been widely reported.

The stem-loop microRNA we studied, which is the precursor of mature microRNA, can be regarded as a reference of mature microRNA helping to better understand the potential molecules of prognostic and diagnostic factors in the progression of LUAD. This mechanism of action can be used for further research on potential drug targets. The quantitative analysis of microRNA expression data is indeed significant for cancer development, validating and demonstrating the power of our framework of dynamical biomarkers research.

Taken together, based on the ncRNA transcriptome, we had developed two frameworks to analyze the processes of identifying microRNA function in LUAD patients. Our analysis had yielded some diagnostic and prognostic factors closely related to the three evolutionary stages of LUAD. The comparative study of these biomarkers provides new insights into understanding cancer mechanisms and identifying targets for further drug development.

## 4 Materials and Methods

### 4.1 Clinical and microRNA expression data of LUAD

A total of 555 samples with the corresponding microRNA expression profile data from The Cancer Genome Atlas (TCGA) were used. We followed the Tumor-Node-Metastasis (TNM) staging criteria for malignant tumors to classify LUAD into four stages. In particular, TNM is a standardized classification system established by the International Association for the Study of Lung Cancer to describe the development of lung cancer in terms of size and spread, where "T" describes the size of the tumor and any spread of cancer into nearby tissues, "N" denotes the spread of cancer to nearby lymph nodes, and "M" stands for metastasis, i.e., the spread of cancer to other parts of the body [Goldstraw et al., 2007]. Detailed in Supplementary Table 4. For our datasets, we integrated the TNM stage III and IV as the later stage. Finally, We had that, of the remaining 542 samples, 273, 120, and 103 are labeled as early, middle, and later stages of LUAD, correspondingly, and 46 are normal samples in diagnosis research. In prognosis analysis, it requires pre-processing samples to match the clinical information and especially with not censored survival time data. Thus, the numbers of LUAD samples are 126, 87, and 77 in three stages respectively. (More details in Supplementary Note 1)

### 4.2 Differential Expression analysis

Fold Change (FC) characterizes the relative expression level of samples of interest to that of the control samples. The individual RNA expression can be seen from the volcano map. We used the R-language "Limma" package to analyze the differentially expressed (DE) microRNA profile data in the three stages of LUAD, with the threshold of  $\log_2$  FC

absolute value for filtering the microRNAs set as 1, while ensuring that their P-value (t-statistic [Phipson et al., 2016], see Supplementary Note 4 for detail) is less than 0.05. So, RNAs with FC greater than 1 correspond to up-regulated genes, while those less than minus 1 to down-regulated genes. For the RNA expression data, the total number of stem-loop microRNAs is 1881. Finally, we then obtained that the numbers in the three stages of LUAD are 127, 130, and 131 respectively, as listed in Supplementary Table 1.

### 4.3 KEGG enrichment analysis

Gene enrichment analysis is a widely used approach to identify biological connections. We performed KEGG enrichment analysis for microRNAs of the LUAD, taking into account the various biological processes in Figures 1C and 4C. In particular, the P-value determines whether any term annotates a specified list of genes at a frequency greater than that which can be expected by chance, as determined by the hypergeometric distribution:

$$p = 1 - \sum_{i=0}^{k-1} \frac{\binom{N-M}{n-i} \binom{M}{i}}{\binom{N}{n}}, \quad (1)$$

where  $N$  is the total number of genes in the background distribution,  $M$  is the number of genes within that distribution that are annotated (either directly or indirectly) to the node of interest,  $n$  is the size of the list of genes of interest, and  $k$  is the number of genes within that list which are annotated to the node. The background distribution by default is all the genes that have an annotation.

### 4.4 Eigenvalue decomposition of microRNA expression data

LUAD sample-RNA expression matrix  $\mathbf{X}$ , the row  $m$  is the number of different LUAD samples, and the column  $n$  is the number of microRNAs.

$$\mathbf{X} = \begin{pmatrix} x_{11} & x_{12} & \dots & x_{1n} \\ x_{21} & x_{22} & \dots & x_{2n} \\ \vdots & \vdots & \ddots & \vdots \\ x_{m1} & x_{m2} & \dots & x_{mn} \end{pmatrix}. \quad (2)$$

Decentralize  $\mathbf{X}$  through minus the average expression value and calculate the Covariance matrix  $\mathbf{C}$ :

$$\mathbf{C} = \frac{\mathbf{X}^T \star \mathbf{X}}{n-1}. \quad (3)$$

We performed eigenvalue decomposition of matrix  $\mathbf{C}$  to obtain eigenvectors that correspond to the projection direction of the reconstructed data in the high-dimensional space. A load of eigenvector corresponds to each microRNA, so these eigenvectors are the preservation of microRNA gene expression characteristic information. The degree of variation was calculated by dividing the variance of each eigenvalue by the sample size  $n-1$ . Then we took the top  $k$  eigenvectors whose degree of variation is greater than 90% to obtain information that retains more than 90% of the original microRNA expression data.

### 4.5 Survival curve analysis

We used the Kaplan-Meier method [Kaplan and Meier, 1958, Kaplan, 1983], a non-parametric method, to estimate survival probability from the observed survival data [Smyth, 2004]. The survival probability as a function of time is calculated according to

$$S(t_i) = S(t_{i-1})(1 - d_i/n_i), \quad (4)$$

where  $n_i$  is the number of patients who were alive before time  $t_i$  and  $d_i$  is the number of death events at  $t_i$ . The estimated probability  $S(t_i)$  is a step function that changes value only at the time  $i$  of each event.

Log-rank tests are applied to carry out univariate analysis of the Kaplan-Meier survival curve, which belongs to the chi-square test, where all time points of the sample survival information are equal (i.e., with weight setting to one).

### 4.6 Mutual Information (MI)

Mutual information is a powerful statistical method for feature selection in machine learning, which reduces the input size of the data set without affecting the most relevant features supporting classification or regression problems. Feature

selection can be performed by finding correlations between random features and mutual information (MI) between two discrete random features  $A = (a_1, a_2, \dots, a_k)$  and  $B = (b_1, b_2, \dots, b_k)$  is defined as

$$I(A, B) = \sum_a \sum_b p(a, b) \log \frac{p(a, b)}{p(a)p(b)}. \quad (5)$$

And when only two random variables are independent, MI equals zero, and a higher value means a higher dependence. In our research, we calculated the MI between each feature vector and the patient survival probability vector respectively and reduced the dimension of the data set by keeping the features with MI greater than 0.

This method can greatly preserve the molecular information related to the prognosis targets. In addition, for the mutual information algorithm, we finally chose a relatively loose threshold to ensure that the potential predictive factors will not be discarded.

#### 4.7 Light Gradient Boosting Machine (LightGBM)

LightGBM is one of the ensemble modelings which is a method of creating strong learners by combining weak learners. It is a decision tree algorithm based on the histogram, which has the advantages of fast operation, high accuracy, strong robustness, and so on. It adopts Gradient-Based One-Side Sampling (GOSS) and pays more attention to the samples with insufficient training without excessively changing the distribution of the original data set, thereby reducing the error and improving the accuracy. At the same time, while ensuring high efficiency, the leaf-by-leaf algorithm with depth limitation is adopted, which avoids over-fitting. Based on the above advantages, LightGBM has been widely used in various machine learning tasks, and it has a very good performance in medical data tasks.

#### 4.8 SHAPley Additive explanation (SHAP)

There are many ways to calculate the importance of the features. Among them, the SHAP value can be viewed through the “Consistent Individualized Feature Attribution for Tree Ensembles” [Lundberg et al., 2018], which has good consistency and accuracy in calculating feature importance. Inspired by cooperative game theory, SHAP constructed an additive explanation model, and all characteristics were regarded as “contributors”. For each prediction sample, the model will generate a prediction value, and the SHAP value is the assigned value of each feature in the sample.

Assuming that sample  $i$  is  $x_i$ , the  $j$ -th feature of sample  $i$  is  $x_{ij}$ , the predicted value of the model for this sample is  $y_i$ , and the baseline of the whole model (usually the average value of the target variables for all samples) is  $y_{base}$ , and the SHAP value follows the following equation.

$$y_i = y_{base} + f(x_{i1}) + f(x_{i2}) + \dots + f(x_{ik}) \quad (6)$$

Where  $f(x_{ij})$  is the SHAP value of  $x_{ij}$ . Intuitively,  $f(x_{ij})$  is the contribution of the first feature in the  $j$ -th sample to the final predicted value  $y_i$ . When  $f(x_{ij}) > 0$ , it means that this feature improves the predicted value and has a positive effect; On the contrary, this feature will lower the predicted value and has a negative impact.

#### 4.9 The framework of analysis

Our articulated framework of dynamical analysis combines the following methods: DE analysis, training classification ML for prognosis, searching for diagnostic factors, KEGG enrichment analysis, and survival analysis. A flow chart of these methods was illustrated in Figure 6. In the section **Materials and Methods**, each of the methods were described.

#### 4.10 Computational packages and database

Data processing and statistical analysis used R language (v.3.5.1) and Python (v.3.9). Analyze DE RNAs using the “Limma” package [Zhao et al., 2018], and plot the heatmap of the enrichment analysis and the Kaplan-Meier survival curves using the “heatmap,” “survival,” and “survminer” packages. In the search for prognostic factors, Python was the main language. “Pandas” and “Matplotlib” were used for data analyzing and visualization; “SKlearn,” “LightGBM,” and “SHAP” for the classifier. The various microRNA-TF networks were visualized via Cytoscape (v3.6.1). Finally, The KEGG functional enrichment analysis used the online tool miEAA (2.0) [Kern et al., 2020].

### 5 Key points

- Through integrating clinical information into the transcripts expression data, we had developed two frameworks to analyze the processes of identifying microRNA clinical function: the unsupervised hierarchical clustering was used to find the diagnostic factors and a classification framework to screen out the prognostic factors.

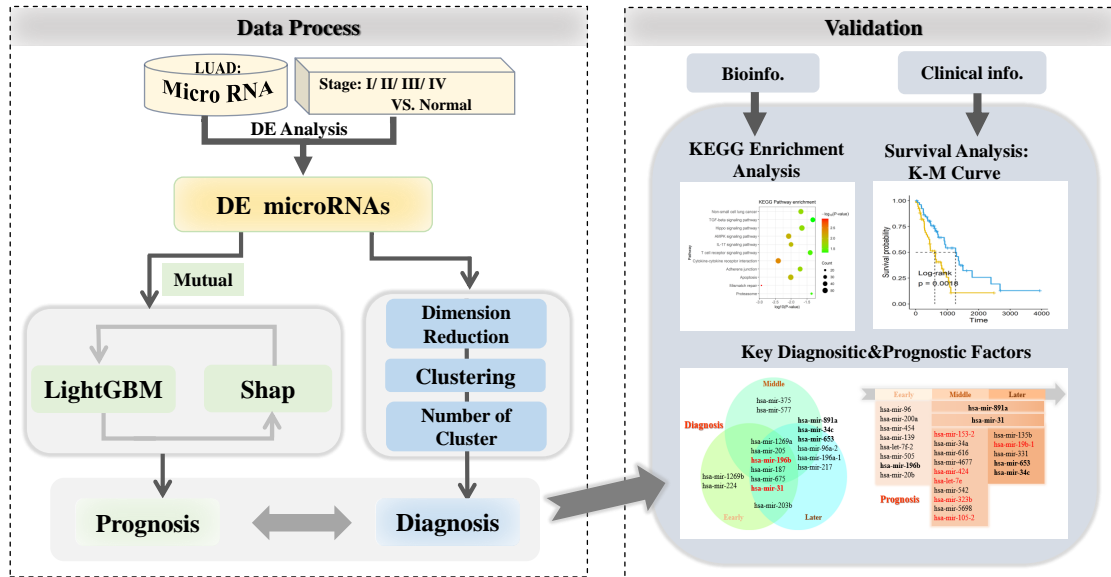


Figure 6: **Overall workflow chart of proposed framework of dynamical biomarkers analysis of lung cancer.** LUAD samples were divided into three stages according to the TNM criteria and analyzed by Differential Expression (DE) microRNAs. Then data reduction, machine learning, and clustering were performed on the gene expression data to uncover the corresponding diagnostic and prognostic factors for each of the three LUAD stages. Statistic analyses about the indicators of algorithms and gene expression characteristics helped to verify these key biomarkers as independent molecular variables (see Supplementary Figures 2 and 3 ). Finally, the microRNA targeted TF network, gene pathway enrichment, and survival analyses were collectively carried out from bioinformatics and clinical data.

- Our analysis delineated the dynamical changes of these key microRNAs in the progression stages from early to later. Beyond that, high molecular heterogeneity was also observed in Stage II in LUAD.
- We found that several microRNAs impact the survival risk of patients and some of them target important TF.
- Five microRNAs (hsa-mir-196b, hsa-mir-31, hsa-mir-891a, hsa-mir-34c, and hsa-mir-653) can markedly serve as not only potential diagnostic factors of stage classification but also prognostic tools in the monitoring of lung cancer.

## 6 Competing interests

There is NO Competing Interest.

## 7 Author contributions statement

Z.-T.B. and Q.-N.Z. designed research; D.K. and K.W. analyzed data and performed research; all authors wrote and reviewed the manuscript.

## 8 Acknowledgments

This work is supported by Energy Science and Technology Guangdong Laboratory (No.HND20TDZLZL00)

## References

- H. Aboutalebi, A. Bahrami, A. Soleimani, N. Saeedi, F. Rahmani, M. Khazaei, H. Fiuji, M. Shafiee, G. A. Ferns, A. Avan, et al. The diagnostic, prognostic and therapeutic potential of circulating micrornas in ovarian cancer. *The international journal of biochemistry & cell biology*, 124:105765, 2020.
- B. D. Adams, A. L. Kasinski, and F. J. Slack. Aberrant regulation and function of microRNAs in cancer. *Curr. Biol.*, 24 (16):R762–R776, 2014.

- B.-C. Ahn, J.-W. So, C.-B. Synn, T. H. Kim, J. H. Kim, Y. Byeon, Y. S. Kim, S. G. Heo, S.-D. Yang, M. R. Yun, et al. Clinical decision support algorithm based on machine learning to assess the clinical response to anti-programmed death-1 therapy in patients with non-small-cell lung cancer. *European Journal of Cancer*, 153:179–189, 2021.
- E. Anastasiadou, L. S. Jacob, and F. J. Slack. Non-coding RNA networks in cancer. *Nat. Rev. Cancer*, 18(1):5, 2018.
- K. Asakura, T. Kadota, J. Matsuzaki, Y. Yoshida, Y. Yamamoto, K. Nakagawa, S. Takizawa, Y. Aoki, E. Nakamura, J. Miura, et al. A mirna-based diagnostic model predicts resectable lung cancer in humans with high accuracy. *Communications biology*, 3(1):1–9, 2020.
- D. P. Bartel. Metazoan micrornas. *Cell*, 173(1):20–51, 2018.
- L. Chen, L. Heikkinen, C. Wang, Y. Yang, H. Sun, and G. Wong. Trends in the development of mirna bioinformatics tools. *Briefings in bioinformatics*, 20(5):1836–1852, 2019.
- E. Dama, T. Colangelo, E. Fina, M. Cremonesi, M. Kallikourdis, G. Veronesi, and F. Bianchi. Biomarkers and lung cancer early detection: State of the art. *Cancers*, 13(15):3919, 2021.
- X. Dong, X. Dan, A. Yawen, X. Haibo, L. Huan, T. Mengqi, C. Linglong, and R. Zhao. Identifying sarcopenia in advanced non-small cell lung cancer patients using skeletal muscle ct radiomics and machine learning. *Thoracic cancer*, 11(9):2650–2659, 2020.
- M. S. Ebert, J. R. Neilson, and P. A. Sharp. MicroRNA sponges: competitive inhibitors of small RNAs in mammalian cells. *Nat. Meth.*, 4(9):721, 2007.
- M. D. Edmonds, K. L. Boyd, T. Moyo, R. Mitra, R. Duszynski, M. P. Arrate, X. Chen, Z. Zhao, T. S. Blackwell, T. Andl, et al. Microrna-31 initiates lung tumorigenesis and promotes mutant kras-driven lung cancer. *The Journal of clinical investigation*, 126(1):349–364, 2016.
- N. J. Epsi, S. Panja, S. R. Pine, and A. Mitrofanova. pathCHEMO, a generalizable computational framework uncovers molecular pathways of chemoresistance in lung adenocarcinoma. *Commun. Biol.*, 2(1):1–13, 2019.
- M. Farsi. Filter-based feature selection and machine-learning classification of cancer data. *INTELLIGENT AUTOMATION AND SOFT COMPUTING*, 28(1):83–92, 2021.
- L. F. Gebert and I. J. MacRae. Regulation of microrna function in animals. *Nature reviews Molecular cell biology*, 20(1):21–37, 2019.
- P. Goldstraw, J. Crowley, K. Chansky, D. J. Giroux, P. A. Groome, R. Rami-Porta, P. E. Postmus, V. Rusch, L. Sobin, I. A. for the Study of Lung Cancer International Staging Committee, et al. The IASLC Lung Cancer Staging Project: proposals for the revision of the TNM stage groupings in the forthcoming (seventh) edition of the TNM Classification of malignant tumours. *J. Thoracic Oncol.*, 2(8):706–714, 2007.
- J. Guinde, D. Frankel, S. Perrin, V. Delecourt, N. Lévy, F. Barlesi, P. Astoul, P. Roll, and E. Kaspi. Lamins in lung cancer: Biomarkers and key factors for disease progression through miR-9 regulation? *Cell*, 7(7):78, 2018.
- H. Hanieh, E. A. Ahmed, R. Vishnubalaji, and N. M. Alajez. Sox4: epigenetic regulation and role in tumorigenesis. In *Seminars in Cancer Biology*, volume 67, pages 91–104. Elsevier, 2020.
- H.-C. Hong, C.-H. Chuang, W.-C. Huang, S.-L. Weng, C.-H. Chen, K.-H. Chang, K.-W. Liao, and H.-D. Huang. A panel of eight micrornas is a good predictive parameter for triple-negative breast cancer relapse. *Theranostics*, 10(19):8771, 2020.
- C. Hou, B. Sun, Y. Jiang, J. Zheng, N. Yang, C. Ji, Z. Liang, J. Shi, R. Zhang, Y. Liu, et al. Microrna-31 inhibits lung adenocarcinoma stem-like cells via down-regulation of met-pi3k-akt signaling pathway. *Anti-Cancer Agents in Medicinal Chemistry (Formerly Current Medicinal Chemistry-Anti-Cancer Agents)*, 16(4):501–518, 2016.
- S.-D. Hsu, Y.-T. Tseng, S. Shrestha, Y.-L. Lin, A. Khaleel, C.-H. Chou, C.-F. Chu, H.-Y. Huang, C.-M. Lin, S.-Y. Ho, et al. miRTarBase update 2014: an information resource for experimentally validated miRNA-target interactions. *Nucl. Acids Res.*, 42(D1):D78–D85, 2014.
- W. Huang, Y. Yan, Y. Liu, M. Lin, J. Ma, W. Zhang, J. Dai, J. Li, Q. Guo, H. Chen, et al. Exosomes with low mir-34c-3p expression promote invasion and migration of non-small cell lung cancer by upregulating integrin  $\alpha 2\beta 1$ . *Signal transduction and targeted therapy*, 5(1):1–13, 2020a.
- X. Huang, S. Xiao, X. Zhu, Y. Yu, M. Cao, X. Zhang, S. Li, W. Zhu, F. Wu, X. Zheng, et al. mir-196b-5p-mediated downregulation of fas promotes nslc progression by activating il6-stat3 signaling. *Cell death & disease*, 11(9):1–13, 2020b.
- Z. Huang, J. Shi, Y. Gao, C. Cui, S. Zhang, J. Li, Y. Zhou, and Q. Cui. Hmdd v3. 0: a database for experimentally supported human microrna–disease associations. *Nucleic acids research*, 47(D1):D1013–D1017, 2019.
- E. L. Kaplan. This week’s citation classic. *Curr. Cont.*, 24:14, 1983.



- E. L. Kaplan and P. Meier. Nonparametric estimation from incomplete observations. *J. Ame. Stat. Asso.*, 53(282): 457–481, 1958.
- A. L. Kasinski and F. J. Slack. MicroRNAs en route to the clinic: progress in validating and targeting microRNAs for cancer therapy. *Nat. Rev. Cancer*, 11(12):849, 2011.
- G. Ke, Q. Meng, T. Finley, T. Wang, W. Chen, W. Ma, Q. Ye, and T.-Y. Liu. Lightgbm: A highly efficient gradient boosting decision tree. *Advances in neural information processing systems*, 30:3146–3154, 2017.
- F. Kern, T. Fehlmann, J. Solomon, L. Schwed, N. Grammes, C. Backes, K. Van Keuren-Jensen, D. W. Craig, E. Meese, and A. Keller. mieaa 2.0: integrating multi-species microRNA enrichment analysis and workflow management systems. *Nucleic acids research*, 48(W1):W521–W528, 2020.
- L. Kozachenko and N. N. Leonenko. Sample estimate of the entropy of a random vector. *Problemy Peredachi Informatsii*, 23(2):9–16, 1987.
- A. Kraskov, H. Stögbauer, and P. Grassberger. Estimating mutual information. *Physical review E*, 69(6):066138, 2004.
- H. Li, C. Feng, and S. Shi. mir-196b promotes lung cancer cell migration and invasion through the targeting of gata6. *Oncology letters*, 16(1):247–252, 2018.
- X. Li, Z. Ren, and J. Tang. Microrna-34a: a potential therapeutic target in human cancer. *Cell death & disease*, 5(7): e1327–e1327, 2014.
- G. Liang, W. Meng, X. Huang, W. Zhu, C. Yin, C. Wang, M. Fassan, Y. Yu, M. Kudo, S. Xiao, et al. mir-196b-5p-mediated downregulation of tspan12 and gata6 promotes tumor progression in non-small cell lung cancer. *Proceedings of the National Academy of Sciences*, 117(8):4347–4357, 2020.
- G. Liu, A. Friggeri, Y. Yang, J. Milosevic, Q. Ding, V. J. Thannickal, N. Kaminski, and E. Abraham. miR-21 mediates fibrogenic activation of pulmonary fibroblasts and lung fibrosis. *J. Exp. Med.*, 207(8):1589–1597, 2010.
- Y. Liu, A. Beyer, and R. Aebersold. On the dependency of cellular protein levels on mRNA abundance. *Cell*, 165(3): 535–550, 2016.
- A. Lopez-Rincon, M. Martinez-Archundia, G. U. Martinez-Ruiz, A. Schoenhuth, and A. Tonda. Automatic discovery of 100-mirna signature for cancer classification using ensemble feature selection. *BMC bioinformatics*, 20(1):1–17, 2019.
- S. M. Lundberg, G. G. Erion, and S.-I. Lee. Consistent individualized feature attribution for tree ensembles. *arXiv preprint arXiv:1802.03888*, 2018.
- S. M. Lundberg, G. Erion, H. Chen, A. DeGrave, J. M. Prutkin, B. Nair, R. Katz, J. Himmelfarb, N. Bansal, and S.-I. Lee. From local explanations to global understanding with explainable ai for trees. *Nature machine intelligence*, 2(1):56–67, 2020.
- S.-S. Luo, X.-W. Liao, and X.-D. Zhu. Genome-wide analysis to identify a novel microRNA signature that predicts survival in patients with stomach adenocarcinoma. *Journal of Cancer*, 10(25):6298, 2019.
- B. Ma, Y. Geng, F. Meng, G. Yan, and F. Song. Identification of a sixteen-gene prognostic biomarker for lung adenocarcinoma using a machine learning method. *Journal of Cancer*, 11(5):1288, 2020.
- J. R. Molina, P. Yang, S. D. Cassivi, S. E. Schild, and A. A. Adjei. Non-small cell lung cancer: Epidemiology, risk factors, treatment, and survivorship. *Mayo Clin. Proc.*, 83(5):584–594, 2008.
- P. Naeli, F. Yousefi, Y. Ghasemi, A. Savardashtaki, and H. Mirzaei. The role of microRNAs in lung cancer: implications for diagnosis and therapy. *Current molecular medicine*, 20(2):90–101, 2020.
- C. G. A. R. Network and Others. Comprehensive molecular profiling of lung adenocarcinoma. *Nature*, 511(7511):543, 2014.
- M. Pandey, A. Mukhopadhyay, S. K. Sharawat, and S. Kumar. Role of microRNAs in regulating cell proliferation, metastasis and chemoresistance and their applications as cancer biomarkers in small cell lung cancer. *Biochimica et Biophysica Acta (BBA)-Reviews on Cancer*, page 188552, 2021.
- B. Phipson, S. Lee, I. J. Majewski, W. S. Alexander, and G. K. Smyth. Robust hyperparameter estimation protects against hypervariable genes and improves power to detect differential expression. *Ann. Appl. Stat.*, 10(2):946, 2016.
- B. Quinto. Next-generation machine learning with spark: Covers xgboost lightgbm spark nlp distributed deep learning with keras and more. *Next-Generation Mach. Learn. with Spark Cover: XGBoost, Light. Spark NLP, Distrib. Deep Learn. with Keras, More*, pages 1–355, 2020.
- B. C. Ross. Mutual information between discrete and continuous data sets. *PloS one*, 9(2):e87357, 2014.

- C. M. Rudin, E. Brambilla, C. Faivre-Finn, and J. Sage. Small-cell lung cancer. *Nature Reviews Disease Primers*, 7(1): 1–20, 2021.
- M. Safran, I. Dalah, J. Alexander, N. Rosen, T. Iny Stein, M. Shmoish, N. Nativ, I. Bahir, T. Doniger, H. Krug, et al. Genecards version 3: the human gene integrator. *Database*, 2010, 2010.
- L. Salmena, L. Poliseno, Y. Tay, L. Kats, and P. P. Pandolfi. A ceRNA hypothesis: the Rosetta Stone of a hidden RNA language? *Cell*, 146(3):353–358, 2011.
- A. A. Sayyed, P. Gondaliya, P. Bhat, M. Mali, N. Arya, A. Khairnar, and K. Kalia. Role of mirnas in cancer diagnostics and therapy: A recent update. *Current pharmaceutical design*, 2021.
- R. Segal, K. Miller, and A. Jemal. Cancer statistics, 2018. *CA Cancer J. Clin.*, 68:7–30, 2018.
- J.-S. Seo, Y. S. Ju, W.-C. Lee, J.-Y. Shin, J. K. Lee, T. Bleazard, J. Lee, Y. J. Jung, J.-O. Kim, J.-Y. Shin, et al. The transcriptional landscape and mutational profile of lung adenocarcinoma. *Geno. Res.*, 22(11):2109–2119, 2012.
- G. Smyth. Linear models and empirical bayes methods for assessing differential expression in microarray experiments. *Stat. Appl. Genet. Mol. Biol.*, 3:3, 2004.
- H. Sung, J. Ferlay, R. L. Siegel, M. Laversanne, I. Soerjomataram, A. Jemal, and F. Bray. Global cancer statistics 2020: Globocan estimates of incidence and mortality worldwide for 36 cancers in 185 countries. *CA: a cancer journal for clinicians*, 71(3):209–249, 2021.
- Y. Tay, F. A. Karreth, and P. P. Pandolfi. Aberrant ceRNA activity drives lung cancer. *Cell Res.*, 24(3):259, 2014a.
- Y. Tay, J. Rinn, and P. P. Pandolfi. The multilayered complexity of ceRNA crosstalk and competition. *Nature*, 505(7483):344, 2014b.
- T. Vergoulis, I. S. Vlachos, P. Alexiou, G. Georgakilas, M. Maragkakis, M. Reczko, S. Gerangelos, N. Koziris, T. Dalamagas, and A. G. Hatzigeorgiou. TarBase 6.0: capturing the exponential growth of miRNA targets with experimental support. *Nucl. Acids Res.*, 40(D1):D222–D229, 2011.
- H.-T. Wei, E.-N. Guo, X.-W. Liao, L.-S. Chen, J.-L. Wang, M. Ni, and C. Liang. Genome-scale analysis to identify potential prognostic microrna biomarkers for predicting overall survival in patients with colon adenocarcinoma. *Oncology reports*, 40(4):1947–1958, 2018.
- K. L. Wu, Y. M. Tsai, C. T. Lien, P. L. Kuo, and J. Y. Hung. The roles of microrna in lung cancer. *International Journal of Molecular Sciences*, 20(7), 2019.
- F. Xiao, Z. Zuo, G. Cai, S. Kang, X. Gao, and T. Li. miRecords: an integrated resource for microRNA–target interactions. *Nucl. Acids Res.*, 37(suppl\_1):D105–D110, 2008.
- B. Xie, Q. Ding, H. Han, and D. Wu. mircancer: a microrna–cancer association database constructed by text mining on literature. *Bioinformatics*, 29(5):638–644, 2013.
- G. Xin, X. Cao, W. Zhao, P. Lv, G. Qiu, Y. Li, B. Wang, B. Fang, and Y. Jia. Microrna expression profile and tnm staging system predict survival in patients with lung adenocarcinoma. *Mathematical Biosciences and Engineering: MBE*, 17(6):8074–8083, 2020.
- H. Yan, H. Cai, Q. Guan, J. He, J. Zhang, Y. Guo, H. Huang, X. Li, Y. Li, Y. Gu, et al. Individualized analysis of differentially expressed mirnas with application to the identification of mirnas deregulated commonly in lung cancer tissues. *Briefings in bioinformatics*, 19(5):793–802, 2018.
- Z. Yang, H. Yin, L. Shi, and X. Qian. A novel microrna signature for pathological grading inlung adenocarcinoma based on tcga and geo data. *International Journal of Molecular Medicine*, 45(5), 2020.
- N. Yu, S. Yong, H. K. Kim, Y.-L. Choi, Y. Jung, D. Kim, J. Seo, Y. E. Lee, D. Baek, J. Lee, et al. Identification of tumor suppressor mirnas by integrative mirna and mrna sequencing of matched tumor–normal samples in lung adenocarcinoma. *Molecular oncology*, 13(6):1356–1368, 2019.
- X. Zhang, L. Ma, L. Zhai, D. Chen, Y. Li, Z. Shang, Z. Zhang, Y. Gao, W. Yang, Y. Li, et al. Construction and validation of a three-microrna signature as prognostic biomarker in patients with hepatocellular carcinoma. *International journal of medical sciences*, 18(4):984, 2021.
- M. Zhao, J. Feng, and L. Tang. Competing endogenous rnas in lung cancer. *Cancer Biology & Medicine*, 18(1):1, 2021.
- Y. Zhao, H. Wang, C. Wu, M. Yan, H. Wu, J. Wang, X. Yang, and Q. Shao. Construction and investigation of lncRNA-associated ceRNA regulatory network in papillary thyroid cancer. *Oncol. Rep.*, 39(3):1197–1206, 2018.
- S. Zhong, H. Golpon, P. Zardo, and J. Borlak. mirnas in lung cancer. a systematic review identifies predictive and prognostic mirna candidates for precision medicine in lung cancer. *Translational Research*, 2020.
- S. Zhong, H. Golpon, P. Zardo, et al. mirnas in lung cancer. a systematic review identifies predictive and prognostic mirna candidates for precision medicine in lung cancer. *Translational Research*, 230:164–196, 2021.